Methanol–Water Aqueous-Phase Reforming with the Assistance of Dehydrogenases at Near-Room Temperature

Yangbin Shen,[a] Yulu Zhan,[a] Shuping Li,[a] Fandi Ning,[a] Ying Du,[a] Yunjie Huang,[b] Ting He,[a] and Xiaochun Zhou*[a, c, d]

As an excellent hydrogen-storage medium, methanol has many advantages, such as high hydrogen content (12.6 wt%), low cost, and availability from biomass or photocatalysis. However, conventional methanol–water reforming usually proceeds at high temperatures. In this research, we successfully designed a new effective strategy to generate hydrogen from methanol at near-room temperature. The strategy involved two main processes: $CH_3OH \rightarrow HCOOH \rightarrow H_2$ and $NADH \rightarrow HCOOH \rightarrow H_2$. The first process ($CH_3OH \rightarrow HCOOH \rightarrow H_2$) was performed by an alcohol dehydrogenase (ADH), an aldehyde dehydrogenase (ALDH), and an Ir catalyst. The second procedure ($NADH \rightarrow HCOOH \rightarrow H_2$) was performed by formate dehydro-genase (FDH) and the Ir catalyst. The Ir catalyst used was a previously reported polymer complex catalyst [Cp*IrCl₂(ppy); Cp* = pentamethylcyclopentadienyl, ppy = polypyrrole] with high catalytic activity for the decomposition of formic acid at room temperature and is compatible with enzymes, coenzymes, and poisoning chemicals. Our results revealed that the optimum hydrogen generation rate could reach up to 17.8 μmol h^{-1} g$_{cat}$$^{-1}$ under weak basic conditions at 30°C. This will have high impact on hydrogen storage, production, and applications and should also provide new inspiration for hydrogen generation from methanol.

Introduction

Environmental problems have seriously threatened the quality of human life. The over exploitation of fossil fuels caused the level of carbon dioxide to exceed 400 ppm in the atmosphere in 2015, and this level will keep increasing over the following years.[1] Such a high carbon dioxide level exceeds any level over the past 2.1 million years.[1] Developing clean energy sources is a promising way to solve these problems. Hydrogen is deemed to be the most promising clean energy source because of its many advantages, which include high energy density (143 MJ kg^{-1}), environmentally friendly products (only

water), abundance on earth, and proven applications in hydrogen–oxygen fuel cells.[2–4]

Although hydrogen has many advantages, its production and storage still face several difficulties that strongly hinder its applications. The storage of high-pressure or liquid hydrogen consumes much energy, which raises costs and results in a loss in the price competitiveness of hydrogen versus fossil energy.

Since organic molecules were reported to be used as H₂ carriers, organic hydrogen-storage technology has become a hot topic in research. Compared with hydrogen-storage tanks, organic compounds have clear advantages, such as higher hydrogen content and lower costs. Moreover, organic compounds can achieve a satisfactory hydrogen conversion rate (Table S1 in the Supporting Information), which makes us believe it will be a mainstream research direction for hydrogen generation.

The generation of hydrogen through photocatalytic water splitting is also a very promising technology for the production of hydrogen in large amounts.[5–8] Nevertheless, it is difficult to use photocatalysis technology to generate hydrogen in moving vehicles or portable devices, because sunlight is usually unavailable on these devices. In general, hydrogen production from methanol–water reforming would be a promising technology that could overcome the difficulties of mass hydrogen generation and cost control.[9–11] Except for these advantages, we should also pay attention to the toxicity of methanol.

However, the conventional methanol–water reforming reaction usually occurs at high temperatures (200–800°C),[9] and produces a high concentration of CO.[12–14] The reforming gas

[a] Dr. Y. Shen, Y. Zhan, S. Li, F. Ning, Y. Du, T. He, Prof. X. Zhou
Division of Advanced Nanomaterials, Suzhou Institute of Nano-tech and Nano-bionics (SINANO)
Chinese Academy of Sciences
Suzhou 215123 (P.R. China)
E-mail: xczhou2013@sinano.ac.cn

[b] Prof. Y. Huang
Faculty of Materials Science and Chemistry
China University of Geosciences
Wuhan 430074 (P.R. China)

[c] Prof. X. Zhou
Key Laboratory of Nanodevices and Applications
Chinese Academy of Sciences
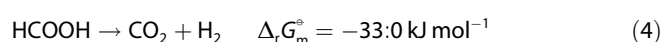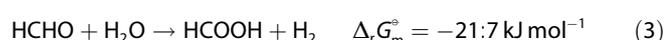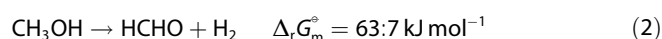Suzhou 215123 (P.R. China)

[d] Prof. X. Zhou
CAS Key Laboratory for Nano-Bio Interface
Suzhou Institute of Nano-Tech and Nano-Bionics
Chinese Academy of Sciences
Suzhou, 215123 (P.R. China)

should be deeply treated with the water–gas-shift (WGS) reaction or selective oxidation to remove CO before application in fuel cells.[15] Consequently, costs and system complexity will increase and make portable applications, such as in hydrogen vehicles, inconvenient. To solve these problems, highly active and selective catalysts were developed to catalyze methanol–water reforming at low temperature (< 100 °C) to produce high-quality H_2 with a trace or without CO.[16,17] The total reaction of methanol–water reforming is proposed and validated as follows [Eq. (1)]:[18–20]

$$CH_3OH + H_2O \rightarrow 3\,H_2 + CO_2 \qquad \Delta_r G_m^{\ominus} = 9.0\,kJ\,mol^{-1} \qquad (1)$$

The above reaction can be divided into three simple reactions:[18–20]

$$CH_3OH \rightarrow HCHO + H_2 \qquad \Delta_r G_m^{\ominus} = 63.7\,kJ\,mol^{-1} \qquad (2)$$

$$HCHO + H_2O \rightarrow HCOOH + H_2 \qquad \Delta_r G_m^{\ominus} = -21.7\,kJ\,mol^{-1} \qquad (3)$$

$$HCOOH \rightarrow CO_2 + H_2 \qquad \Delta_r G_m^{\ominus} = -33.0\,kJ\,mol^{-1} \qquad (4)$$

From Reactions (2), (3), and (4), we can find that the first step for methanol dehydrogenation is a Gibbs's free energy increasing process [Reaction (2)], whereas the following formaldehyde and formic acid dehydrogenation steps are Gibbs's free energy decreasing processes at room temperature. The high energy barrier of Reaction (2) makes the whole methanol–water reforming reaction difficult, even though the following reactions can be easily realized at low temperatures.[21–25] To promote the first methanol dehydrogenation step, alkaline reagents can be added to the reaction system.[16,20,26,27] However, generated CO_2 neutralizes the alkaline solution, and hydrogen generation stops after the alkali is exhausted. Even if such an alkaline reagent is conducive to the reaction, the reaction temperature is still much higher than room temperature.

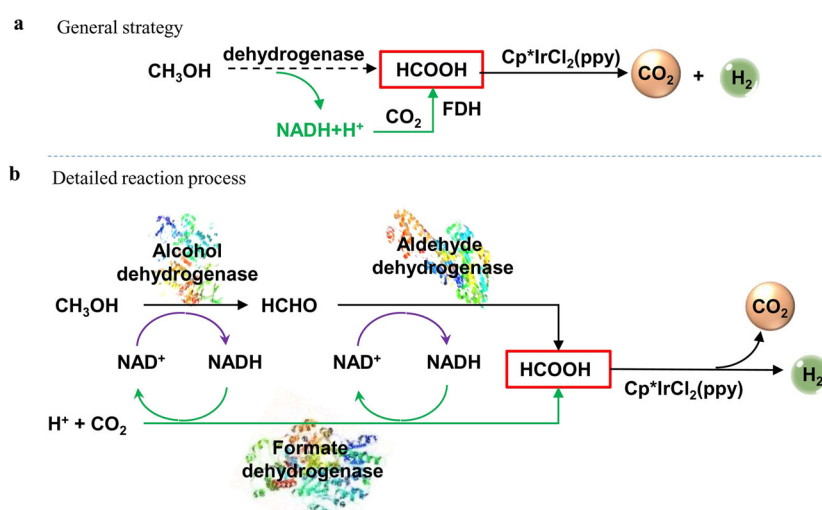So far, it is still a great challenge to produce hydrogen from methanol–water reforming at near-room temperature. Recent-ly, some exciting results were achieved through photocatalysis, electrocatalysis, and bioinduced catalysis.[17,28–31] These procedures, however, needed a continuous supply of extra energy or oxygen. Nonetheless, methanol–water reforming could be realized at near-room temperature without any assistance of extra energy or additives under ideal conditions.

Moreover, huge progress has been made in hydrogen production from the dehydrogenation of formic acid. It was reported that formic acid could be effectively decomposed to hydrogen by various homogenous and heterogeneous catalysts at room temperature.[21,22,32,33] Therefore, hydrogen production from methanol could be realized if methanol could be well converted into formic acid. In this work, we successfully designed a novel pathway to convert methanol into formic acid, which underwent catalytic decomposition to hydrogen at near-room temperature. The conversion of methanol into formic acid was realized by two dehydrogenases, including an alcohol dehydrogenase (ADH) and an aldehyde dehydrogenase (ALDH). The decomposition of formic acid to hydrogen was performed by using a previously reported polymer complex catalyst, Cp*IrCl₂(ppy) (Cp* = pentamethylcyclopentadienyl, ppy = polypyrrole).[34] During the process, generated NADH was catalytically dehydrogenated by formate dehydrogenase (FDH) to produce formic acid. The three dehydrogenases and the catalyst synergistically and efficiently catalyzed the generation of hydrogen from methanol at near-room temperature.

Results and Discussion

Pathway design

In this research, methanol was successfully converted into formic acid by the cooperation of two dehydrogenases (Scheme 1a). Then, formic acid was catalytically decomposed to H_2 and CO_2 by Cp*IrCl₂(ppy), which we already proved to have high catalytic activity and selectivity for the decomposition of formic acid.[34] The dehydrogenation of formic acid was

Scheme 1. a) General strategy and b) detailed reaction process to generate H_2 from methanol. Black arrows indicate the methanol dehydrogenation procedure (CH₃OH→HCOOH→H₂). Green arrows indicate CO_2 hydrogenation (CO₂→HCOOH).

↖↖ **These are not the final page numbers!**

the only process for hydrogen generation from methanol throughout the entire strategy.

As exhibited in Scheme 1b, the total process for hydrogen generation from methanol needs three dehydrogenases and the Ir catalyst. Black arrows point to the methanol dehydrogenation process by the alcohol dehydrogenase, aldehyde dehydrogenase, and NAD$^+$. Formic acid and NADH are produced during the reactions [Reactions (5) and (6)]. NAD$^+$ is nicotinamide adenine dinucleotide, which is the coenzyme for the alcohol dehydrogenase and aldehyde dehydrogenase, and NADH is the reduced form of NAD$^+$.

$$CH_3OH + NAD^+ \xrightarrow{ADH} NADH + HCHO + H^+ \tag{5}$$

$$HCHO + H_2O + NAD^+ \xrightarrow{ALDH} NADH + HCOOH + H^+ \tag{6}$$

Then, hydrogen is generated from the decomposition of formic acid, which is catalyzed by Cp*IrCl$_2$(ppy). Formic acid is a key intermediate product [Reaction (7)]:

$$HCOOH \xrightarrow{Ir\ catalyst} H_2 + CO_2 \tag{7}$$

During the dehydrogenation process of methanol and formaldehyde, NAD$^+$ is sacrificed and produces NADH continuously (purple arrows in Scheme 1b). Continuous accumulation of NADH has a negative influence on both methanol dehydrogenation and formic acid generation. Because NAD$^+$ is the key coenzyme for the alcohol dehydrogenase and aldehyde dehydrogenase, we employed formate dehydrogenase to convert NADH into NAD$^+$, which was accompanied by formic acid generation (green arrows in Scheme 1b). This is the CO$_2$ hydrogenation process [Reaction (8)]:[35]

$$NADH + H^+ + CO_2 \xrightarrow{FDH} NAD^+ + HCOOH \tag{8}$$
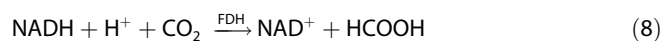
Not only did we make the reaction system continuously work through this method, but we also indirectly generated more hydrogen from NADH. Therefore, this method converts methanol into hydrogen absolutely through ingenious design (Scheme 1). As the enzymes and the Ir catalyst could work at room temperature, hydrogen production from methanol could be realized under mild condition (Figure S1).

Reaction activities of the dehydrogenases at different substrate concentrations

As shown in Scheme 1, the enzymes played an important role during methanol dehydrogenation and formic acid generation. So, research of the enzymes is necessary to help us evaluate the feasibility of hydrogen generation through the designed process outlined in Scheme 1. Additionally, this research would also contribute to determining the substrate concentration in the initial reaction solution, such as the concentrations of methanol and KHCO$_3$. One unit (U) is defined as the amount of enzyme that catalyzes the conversion of 1 micromole (µmol) substrate per minute. There are great differences in the purities of enzymes among different suppliers, so the enzyme activity

based on unit is convenient for different research groups to repeat experiments and to compare the catalytic activity.

Figure 1a shows the variation in the UV/Vis absorbance spectra of NADH over time during methanol dehydrogenation, which is indicative of the catalytic dehydrogenation of methanol by the ADH [Reaction (5)]. Moreover, the dehydrogenation rate was greatly affected by the concentration of CH$_3$OH. Figure 1b shows that the initial dehydrogenation rate increased rapidly at low concentrations of methanol and then reached a saturation value (44.9 µmol min^{-1} g$_{ADH}^{-1}$) at high concentrations of methanol (>260 mm). This saturation concentration is also consistent with the Michaelis constant (130 mm) of the ADH for methanol. To achieve a high and stable reaction rate for the catalytic dehydrogenation of CH$_3$OH by ADH, the CH$_3$OH concentration should be higher than 260 mm. Therefore, 400 mm CH$_3$OH was typically used in the following research.

Figure 1c exhibits the reaction rate for HCHO dehydrogenation at different HCHO concentrations. The reaction rate for HCHO dehydrogenation shows a volcano shape versus HCHO concentration. The peak dehydrogenation rate reaches 8.61 µmol min^{-1} g$_{ALDH}^{-1}$ at 1.01 mm HCHO. At HCHO concentrations lower than 1.01 mm, the reaction rate increased with an increase in the HCHO concentration. However, the reaction rate decreased dramatically if the HCHO concentration exceeded 1.01 mm, which indicated that a high concentration of HCHO inhibited the catalytic activity of the ALDH. In addition, we found that too much HCHO also inhibited the catalytic activity of ADH and FDH (Figures S2 and S3), because a high concentration of HCHO damaged the protein irreversibly and resulted in a loss of protein activity.

We employed FDH to convert NADH back into NAD$^+$ and to produce formic acid simultaneously [Reaction (8)]. Figure 1d shows the variation in the UV/Vis absorbance spectra of NADH over time during the hydrogenation of CO$_2$, which is indicative of the production of formic acid by FDH. Figure 1e shows that the reaction rate increased drastically with an increase in the KHCO$_3$ concentration and then reached a stable reaction rate (1.66 µmol min^{-1} kU^{-1}) after the KHCO$_3$ concentration exceeded 20 mm. To accelerate the initial reaction rate of the total process, 20 mm KHCO$_3$ was usually added in the reaction solution to favor Reaction (8).[36–39]

Critical catalyst for formic acid decomposition

As shown in Scheme 1, the Ir catalyst is critically important for hydrogen generation from the decomposition of formic acid. Unlike ordinary formic acid decomposition in water, the Ir catalyst needs to work in a much more complex solution containing formaldehyde, enzymes, a coenzyme, and glutathione. To make the whole reaction system work effectively, the Ir catalyst should have many unique characteristics. First, the Ir catalyst should have high catalytic activity at low temperature. Second, the activity of the Ir catalyst should not be inhibited by enzymes, the coenzyme, or poisoning chemicals (e.g., glutathione, thiols, cysteine, or mercaptosuccinic acid). Third, the Ir catalyst should have no negative effect on the enzymes and
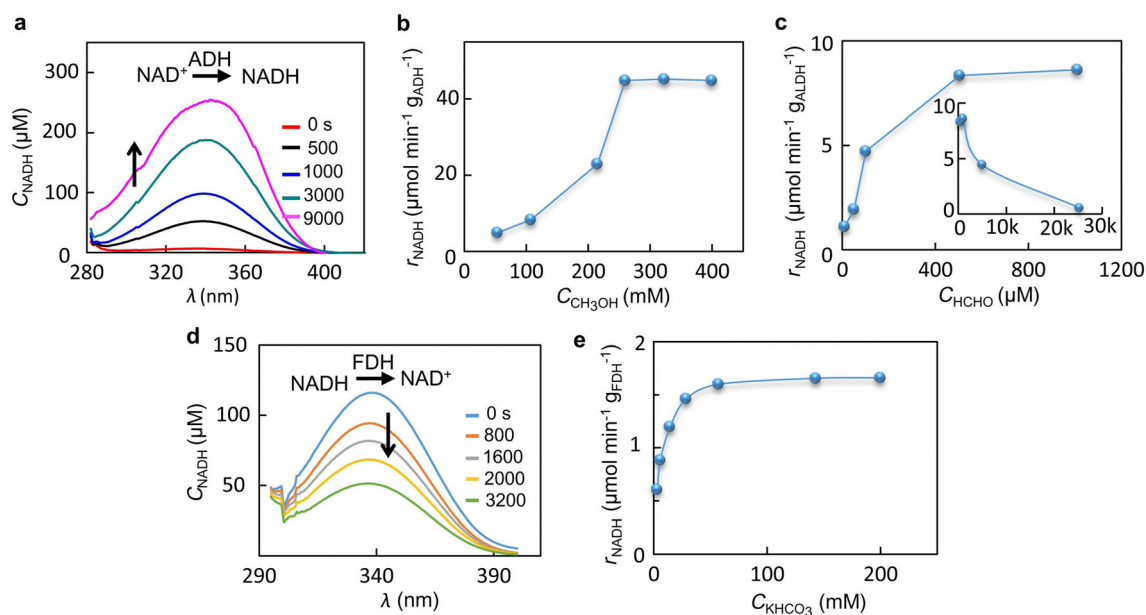
These are not the final page numbers! ↗↗

Figure 1. Catalytic activity of ADH, ALDH, and FDH. a) Variation in the UV/Vis absorbance spectra of NADH versus time during methanol dehydrogenation by ADH. Conditions: pH 8.4, 400 mm CH_3OH, 30 U ADH, 400 µm NAD^+. b) Reaction rate of CH_3OH dehydrogenation at different CH_3OH concentrations. Conditions: 346 µm NAD^+, 16 U ADH, pH 9.0. c) Reaction rate of HCHO dehydrogenation by ALDH at different HCHO concentrations. Conditions: 159 µm NAD^+, 0.63 U ADLH, pH 8.4. d) Variation in the UV/Vis absorbance spectra of NADH versus time during CO_2 catalytic hydrogenation to HCOOH by the FDH. Conditions: 120 µm NADH, 8 U FDH, 3 mm $KHCO_3$, pH 5.8. e) Reaction rate of CO_2 catalytic hydrogenation by the FDH at different $KHCO_3$ concentrations. Conditions: 130 µm NADH, 8 U FDH, pH 7.3. All experiments were performed in phosphate buffer (500 µL) at 25 °C.

coenzyme in the reaction system. In brief, the Ir catalyst must have high activity and compatibility.

Although we have reported many catalysts for the efficient decomposition of formic acid since 2008,[21, 32, 33, 40] those catalysts do not possess all of the abovementioned characteristics. For example, glutathione and mercaptosuccinic acid are poisonous to many metal catalysts, whereas these sulfhydryl compounds are essential to activate the ALDH.[41] Additionally, generated formaldehyde can also poison metal catalysts. Therefore, we employed the reported polymer complex catalyst Cp*IrCl₂(ppy), which possesses high catalytic activity and selectivity for formic acid decomposition[34] (Scheme 2). The Cp*IrCl₂(ppy) catalyst was synthesized through the procedure shown in Scheme 2 (see Figure S4 for details).

Figure 2a shows a typical transmission electron microscopy (TEM) image of the Cp*IrCl₂(ppy) catalyst. No metal nanoparti-
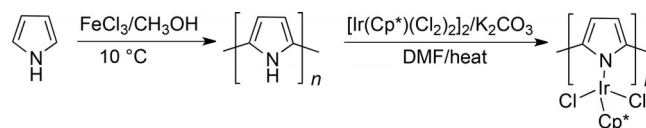
Scheme 2. Schematic illustration for the synthesis of Cp*IrCl₂(ppy).

cles could be found on the surface of the catalyst. The morphology of Cp*IrCl₂(ppy) is similar to that of the as-synthesized polypyrrole precursor (Figure S5a) but is clearly difference from that of polypyrrole-supported Ir nanoparticles (Figure S5c). Figure 2b shows that Cp*IrCl₂(ppy) has high catalytic activity for formic acid decomposition, as it can achieve an initial turnover frequency (TOF) of 725 h^{-1} at 35 °C and can retain high catalytic activity for at least 700 min; the conversion rate of formic acid was 39.6% after 700 min. Moreover, Figure 2c
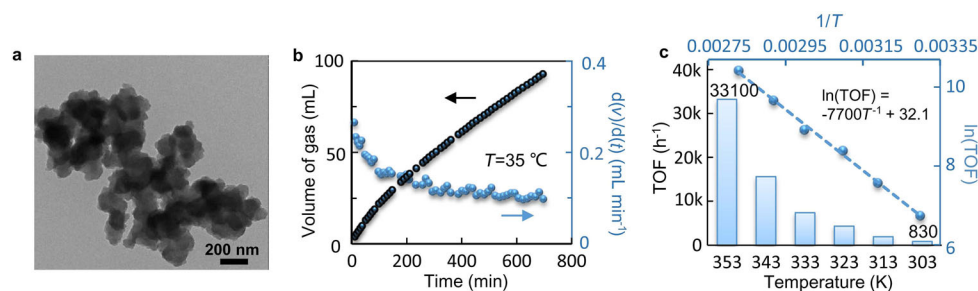

Figure 2. Morphology and catalytic activity of Cp*IrCl₂(ppy). a) TEM image of Cp*IrCl₂(ppy). b) Gas evolution in 1.0 m HCOOH catalyzed by Cp*IrCl₂(ppy) (2.3 mg) versus time. c) TOF values and Arrhenius plot at different temperatures, [HCOOH] = 1.0 m, [HCOOH]/[HCOONa] = 1. The amount of catalyst used in the reaction was 4.0 mg, and the reaction solution was 5 mL.

↖↖ **These are not the final page numbers!**

shows that the TOF of Cp*IrCl$_2$(ppy) reaches up to 33 100 h^{-1} at 80°C. Ln(TOF) has a linear relationship with 1/T, and consequently, the activation energy (E_a) of the reaction was calculated to be (64.0±3.6) kJ mol^{-1}. This value is close to that of previously reported homogenous catalysts containing the Ir(Cp*) group,[25,42] which indicates that Cp*IrCl$_2$(ppy) has a similar active site for HCOOH dehydrogenation.

To prove that the Ir catalyst had no negative effect on the enzymes or coenzyme, we mixed Cp*IrCl$_2$(ppy) with the ADH, ALDH, and FDH for 12 h before measuring the activities of the enzymes. The enzymes maintained their original catalytic activities for their respective reactions (Figure S4). Therefore, the Ir Cp*IrCl$_2$(ppy) catalyst had no negative effect on the activities of the ADH, ALDH, and FDH.

Why does Cp*IrCl$_2$(ppy) have so many unique characteristics? We can attribute these characteristics to the unique structure and composition of Cp*IrCl$_2$(ppy). First, Cp*IrCl$_2$(ppy) is a kind of complex catalyst that has high activity and selectivity for HCOOH dehydrogenation. Second, the catalytic iridium core is strongly capped by Cp* and polypyrrole, which prevents catalyst poisoning by enzymes, coenzymes, and chemicals in the reaction solution. Third, the TEM image shows that Cp*IrCl$_2$(ppy) has an amorphous structure that is inherited from polypyrrole. The average pore size of Cp*IrCl$_2$(ppy) is 11.4 nm (Figure S6). The porous structure provides highly efficient access for mass transfer during HCOOH dehydrogenation. Fourth, polypyrrole is a thermally stable polymer that is insoluble in most common solvents and has fine biological compatibility. Therefore, it is widely used in many fields, such as in lithium storage, CO$_2$ capture, Li$_2$S cathodes, electrochemical reduction of carbon dioxide, hydrogen peroxide decomposition, and so on.[42–49] Hence, the Ir catalyst will not interact with the active site of the enzymes and shows high compatibility with enzymes.

Hydrogen generation from methanol at near-room temperature

Every ingredient in the reaction system is necessary to ensure continuous hydrogen generation from methanol (Figure 3 a). To study the roles of the enzymes and catalyst in Scheme 1 to prove that all of the enzymes and catalyst were necessary, we performed a series of control experiments. Each experiment lacked one ingredient compared with the standard experiment in Figure 3 a.

As hydrogen is only generated from the decomposition of formic acid, the dehydrogenation of methanol is the most important step of the total process. Methanol was not converted into formaldehyde by the ADH, and as such, none of the subsequent reactions occurred. Consequently, no hydrogen was generated through the decomposition of formic acid (Figure 3 b).

In the absence of the ALDH, formic acid was not generated from the dehydrogenation of formaldehyde, but NADH generated from the dehydrogenation of methanol could react with CO$_2$ and H$^+$ through catalysis by the FDH in solution, and this process could also theoretically produce formic acid. However,
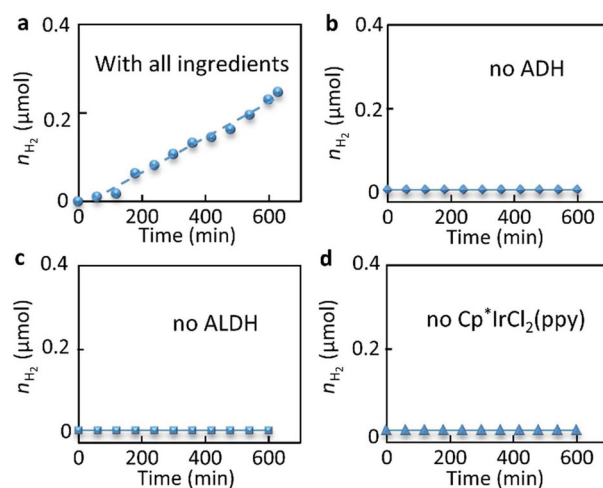

Figure 3. H$_2$ generation from methanol. a) H$_2$ generation under standard condition. Standard conditions without b) ADH, c) ALDH, or d) Cp*IrCl$_2$(ppy). Standard conditions: phosphate buffer (pH 7.75, 5 mL) containing 400 mm CH$_3$OH, 20 mm KHCO$_3$, 4 mm NAD$^+$, Ir catalyst (4 mg), 50 U FDH, 1 U ALDH, and 30 U ADH, N$_2$ atmosphere, 30°C. n(H$_2$O)/n(CH$_3$OH) = 137.5.

no hydrogen was detected by GC even after 600 min (Figure 3 c). Consequently, formic acid production through CO$_2$ hydrogenation was not very efficient in the absence of the ALDH, whereas in our previous research, the process was efficient (Figure 1 d). This was because generated formaldehyde lowered the catalytic activity of the FDH (Figure S4). Actually, HCHO is a nightmare for many enzymes, and a high concentration of formaldehyde even decreased the catalytic activity of the ALDH (Figure 1 c), not to mention those of the ADH and FDH (Figures S2 and S3). In our previous work, we employed chemical catalysts to convert NADH into NAD$^+$ and hydrogen directly, but their catalytic activity was not inhibited by formaldehyde. Therefore, a trace amount of hydrogen was detected after 350 min through the dehydrogenation of NADH.[34]

If Cp*IrCl$_2$(ppy) was missing, although formic acid was generated continuously, it was not catalytically decomposed into CO$_2$ and H$_2$. The decomposition of formic acid is the only method for hydrogen generation. Accordingly, no hydrogen was detected under these conditions (Figure 3 d). As we reported in previous work, if NADH was converted into NAD$^+$ and H$_2$ directly, the hydrogen concentration increased slowly after 200 min,[34] because the decomposition of formic acid was no longer the only method to generate hydrogen in this process. Hydrogen generation from the dehydrogenation of NADH is the other choice.

The dehydrogenation of NADH is the key step for continuous hydrogen generation. In this experiment, we employed the FDH for the conversion of NADH. If we did not take any measures to convert NADH, a trace amount of hydrogen was detected at the beginning of the reaction, but hydrogen was not generated continuously,[34] because NAD$^+$ was a necessary coenzyme for the ADH and ALDH. Continuous consumption of NAD$^+$ decreased the reaction rates for the dehydrogenation of methanol and formaldehyde, and the decomposition rate of formic acid was indirectly affected.

These are not the final page numbers! ↗↗

Effect of temperature on hydrogen generation from methanol

Enzymes are sensitive to reaction conditions, such as temperature, pH, and substrate concentration. As shown in Figure 1b, if the methanol concentration exceeded 260 mM, the reaction rate was optimal. Therefore, we only took the temperature and pH into consideration for hydrogen generation from methanol.

Figure 4a shows hydrogen generation from methanol versus time at different temperatures in phosphate buffer (pH 7.50). Hydrogen continuously evolved for more than 600 min, which proved that this strategy could effectively work under mild reaction conditions. Because the amount of generated hydrogen was linearly related to the reaction time, the whole system reached a steady reaction state. The reaction rate was calculated by fitting the curve with a linear function. Then, the hydrogen generation rate was evaluated by the masses of the enzymes and the Ir catalyst. For example, the hydrogen generation rate was 17.8 $\mu mol\,h^{-1}\,g_{cat}^{-1}$ at 30 °C, which implied that the reaction solution generated 17.8 μmol hydrogen per hour and per gram enzymes and Cp*IrCl$_2$(ppy).

Figure 4b shows that hydrogen production was strongly affected by the reaction temperature. Two optimum temperatures appeared at 25 and 30 °C in the temperature-dependent activity measurements. The optimum temperatures were mainly attributed to the different optimum working temperatures of the enzymes (i.e., ADH, ALDH, and FDH) and the Cp*IrCl$_2$(ppy) catalyst. The first optimum temperature at 25 °C was consistent with the optimum working temperature of ADH and ALDH ($\approx$25 °C provided by Sigma–Aldrich). The second optimum temperature at 30 °C was a compromise and was jointly determined by the three enzymes and the Ir catalyst, because the optimum working temperature of the FDH was up to 36 °C (provided by the FDH supplier). In addition, a higher temperature could favor the decomposition of formic acid (Figure 2c), which is the direct step for hydrogen generation. The highest hydrogen generation rate of 17.8 $\mu mol\,h^{-1}\,g_{cat}^{-1}$ was achieved at 30 °C.

Effect of pH value on hydrogen production from methanol

As all of the enzymes have their own optimum pH conditions, the pH value may have a great influence on hydrogen generation. Figure 5a shows that hydrogen was generated continuously for more than 600 min. Attributable to the mild reaction conditions, the reaction rate did not decrease evidently. The maximum catalytic activity appeared at pH 7.5, and the corresponding hydrogen generation rate was 17.8 $\mu mol\,h^{-1}\,g_{cat}^{-1}$.

The respective optimum pH values of the enzymes and catalyst jointly determined the optimum working pH values for hydrogen generation from methanol. Figure 5c,d shows that the activities of the ADH and ALDH increased upon increasing the pH value, which indicated that the ADH and ALDH preferred weak basic conditions for the dehydrogenation of methanol and formaldehyde, respectively. However, Figure 5e,f shows that the activities of the FDH and the Ir catalyst decreased upon increasing the pH value, which indicated that the FDH and Ir catalyst preferred weak acidic conditions for CO_2 hydrogenation and formic acid decomposition, respectively.[50] Therefore, the hydrogen generation rate of the whole reaction system reached a maximum value at an optimum pH value. In this research, the optimum pH value appears near neutral conditions, that is, pH 7.5.

Conclusions

In this work, we successfully designed a strategy for the complete conversion of methanol into hydrogen at near-room temperature. The strategy involved two processes: $CH_3OH \rightarrow HCOOH \rightarrow H_2$ and $NADH \rightarrow HCOOH \rightarrow H_2$. In the first process ($CH_3OH \rightarrow HCOOH \rightarrow H_2$), methanol was converted into formic acid by the cooperation of two dehydrogenases, they are alcohol dehydrogenase (ADH) and aldehyde dehydrogenase (ALDH). Then, formic acid was dehydrogenated to H_2 and CO_2 by Cp*IrCl$_2$(ppy) (Cp* = pentamethylcyclopentadienyl, ppy = polypyrrole), which is a kind of polymer complex catalyst for formic acid dehydrogenation. Moreover, the dehydrogenation of methanol and formaldehyde consumed NAD$^+$ and generated more NADH. Thus, in the second process (NADH $\rightarrow$ HCOOH $\rightarrow$ H$_2$), we employed formate dehydrogenase (FDH) to
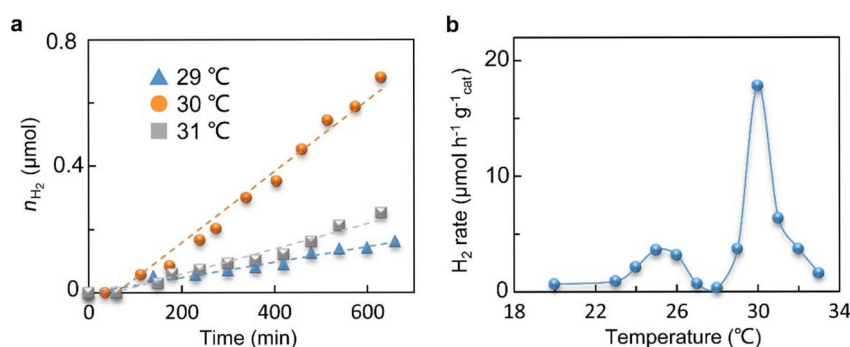

Figure 4. Effect of temperature on H$_2$ generation from methanol. a) H$_2$ production versus time at three different temperatures. b) Effect of temperature on H$_2$ generation rate. The reaction was performed in phosphate buffer (pH 7.5, 5 mL) containing 400 mM CH$_3$OH, 20 mM KHCO$_3$, 4 mM NAD$^+$, Ir catalyst (4.0 mg), 50 U FDH, 1 U ALDH, and 30 U ADH. The reaction was protected under a N$_2$ atmosphere. $n(H_2O)/n(CH_3OH) = 137.5$.
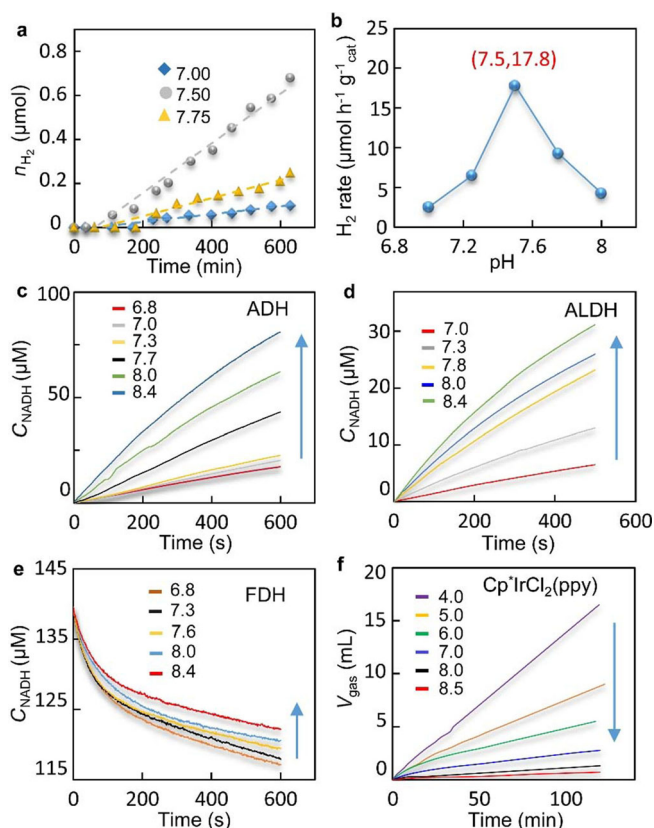
↖↖ **These are not the final page numbers!**

Figure 5. Effect of pH value on H_2 generation from methanol. a) H_2 production versus time at three pH values. b) Effect of pH on H_2 generation rate. Conditions: phosphate buffer (5 mL) containing 400 mm CH_3OH, 20 mm $KHCO_3$, 4 mm NAD^+, Ir catalyst (4 mg), 50 U FDH, 1 U ALDH, and 30 U ADH, N_2 atmosphere, 30 °C. c) Effect of pH on the catalytic activity of the ADH. Conditions: 400 µm NAD^+, 400 mm CH_3OH, phosphate buffer (500 µL), 30 U ADH, 25 °C. d) Effect of pH on the catalytic activity of the ALDH. Conditions: 159 µm NAD^+, 506 µm HCHO, phosphate buffer (500 µL), 0.63 U ADLH, 25 °C. e) Effect of pH on the activity of the FDH for CO_2 hydrogenation. Conditions: 130 µm NADH, 3 mm $KHCO_3$, phosphate buffer (500 µL), 8 U FDH, 25 °C. f) Effect of pH on the activity of the catalyst for HCOOH dehydrogenation. Conditions: 2 m HCOOH, Ir catalyst (4 mg), 30 °C, 5 mL reaction solution. The arrows in panels c–f indicate the direction of increasing pH values.

convert NADH back into NAD^+ and to convert CO_2 into HCOOH simultaneously. Then, formic acid was decomposed to hydrogen and CO_2 by the Ir catalyst. As the enzymes and the Ir catalyst worked at room temperature, hydrogen production from methanol could be achieved under mild conditions. This research also revealed that the hydrogen generation rate was strongly affected by the reaction temperature and pH value. The optimum temperature and pH appeared at 30 °C and 7.50 respectively, and the corresponding hydrogen generation rate reached up to 17.8 µmol h^{-1} g$_{cat}^{-1}$. The optimum temperature and pH value were attributed to the different optimum working temperatures and pH values of the enzymes (i.e., ADH, ALDH, and FDH) and the Ir catalyst. The strategy in this research should inspire other methods for hydrogen production from small organic molecules (e.g., ethanol and ethylene glycol) or biomass (e.g. glucose, starch, and cellulose). The results and knowledge obtained from this research should have a large impact on hydrogen storage, production, and applications.

[1] World Metereological Organization, *The State of Greenhouse Gases in the Atmosphere Based on Global Observations through 2015*, WMO Greenhouse Gas Bulletin, **2016**, http://library.wmo.int/opac/doc_num.php?explnum_id = 3084.

[2] J. A. Rollin, J. M. del Campo, S. Myung, F. Sun, C. You, A. Bakovic, R. Castro, S. K. Chandrayan, C.-H. Wu, M. W. W. Adams, R. S. Senger, Y. H. P. Zhang, *Proc. Natl. Acad. Sci. USA* **2015**, *112*, 4964–4969.

[3] C.-W. Zhang, L.-B. Xu, J.-F. Chen, *Chin. Chem. Lett.* **2016**, *27*, 832–836.

[4] L. Zou, J. Li, T. Yuan, Y. Zhou, X. Li, H. Yang, *Nanoscale* **2014**, *6*, 10686–10692.

[5] T. Hisatomi, J. Kubota, K. Domen, *Chem. Soc. Rev.* **2014**, *43*, 7520–7535.

[6] F. E. Osterloh, *Chem. Soc. Rev.* **2013**, *42*, 2294–2320.

[7] L. Liao, Q. Zhang, Z. Su, Z. Zhao, Y. Wang, Y. Li, X. Lu, D. Wei, G. Feng, Q. Yu, X. Cai, J. Zhao, Z. Ren, H. Fang, F. Robles-Hernandez, S. Baldelli, J. Bao, *Nat. Nanotechnol.* **2014**, *9*, 69–73.

[8] J. Liu, Y. Liu, N. Liu, Y. Han, X. Zhang, H. Huang, Y. Lifshitz, S.-T. Lee, J. Zhon, Z. Kang, *Science* **2015**, *347*, 970–974.

[9] D. R. Palo, R. A. Dagle, J. D. Holladay, *Chem. Rev.* **2007**, *107*, 3992–4021.

[10] A. Monney, E. Barsch, P. Sponholz, H. Junge, R. Ludwig, M. Beller, *Chem. Commun.* **2014**, *50*, 707–709.

[11] X. Yang, *ACS Catal.* **2014**, *4*, 1129–1133.

[12] R. González-Gil, C. Herrera, M. Á. Larrubia, P. Kowalik, I. S. Pieta, L. J. Alemany, *Int. J. Hydrogen Energy* **2016**, *41*, 19781–19788.

[13] F. Wang, G. Wang, *Int. J. Hydrogen Energy* **2016**, *41*, 16835–16841.

[14] F. Ahmadi, M. Haghighi, H. Ajamein, *J. Mol. Catal. A* **2016**, *421*, 196–208.

[15] M. J. Lee, J. S. Kang, Y. S. Kang, D. Y. Chung, H. Shin, C. Y. Ahn, S. Park, M. J. Kim, S. Kim, K. S. Lee, Y. E. Sung, *ACS Catal.* **2016**, *6*, 2398–2407.

[16] J. Campos, L. S. Sharninghausen, M. G. Manas, R. H. Crabtree, *Inorg. Chem.* **2015**, *54*, 5079–5084.

[17] A. Naldoni, M. D'Arienzo, M. Altomare, M. Marelli, R. Scotti, F. Morazzoni, E. Selli, V. Dal Santo, *Appl. Catal. B* **2013**, *130*, 239–248.

[18] R. E. Rodríguez-Lugo, M. Trincado, M. Vogt, F. Tewes, G. Santiso-Quinones, H. Gruetzmacher, *Nat. Chem.* **2013**, *5*, 342–347.

[19] E. A. Bielinski, M. Förster, Y. Zhang, W. H. Bernskoetter, N. Hazari, M. C. Holthausen, *ACS Catal.* **2015**, *5*, 2404–2415.

[20] K.-i. Fujita, R. Kawahara, T. Aikawa, R. Yamaguchi, *Angew. Chem. Int. Ed.* **2015**, *54*, 9057–9060; *Angew. Chem.* **2015**, *127*, 9185–9188.

[21] X. Zhou, Y. Huang, W. Xing, C. Liu, J. Liao, T. Lu, *Chem. Commun.* **2008**, 3540–3542.

[22] J. F. Hull, Y. Himeda, W.-H. Wang, B. Hashiguchi, R. Periana, D. J. Szalda, J. T. Muckerman, E. Fujita, *Nat. Chem.* **2012**, *4*, 383–388.

[23] Y. Im, S. Kang, K. M. Kim, T. Ju, G. B. Han, N. K. Park, T. J. Lee, M. Kang, *Int. J. Photoenergy* **2013**, 452542.

[24] L. E. Heim, S. Vallazza, D. van der Waals, M. H. G. Prechtl, *Green Chem.* **2016**, *18*, 1469–1474.

These are not the final page numbers! ↗↗

[25] S. Fukuzumi, T. Kobayashi, T. Suenobu, *J. Am. Chem. Soc.* **2010**, *132*, 1496 – 1497.

[26] E. Alberico, P. Sponholz, C. Cordes, M. Nielsen, H. J. Drexler, W. Baumann, H. Junge, M. Beller, *Angew. Chem. Int. Ed.* **2013**, *52*, 14162 – 141626; *Angew. Chem.* **2013**, *125*, 14412 – 14416.

[27] P. Hu, Y. Diskin-Posner, Y. Ben-David, D. Milstein, *ACS Catal.* **2014**, *4*, 2649 – 2652.

[28] J. González-Cobos, V. J. Rico, A. n. R. González-Elipe, J. L. Valverde, A. de Lucas-Consuegra, *ACS Catal.* **2016**, *6*, 1942 – 1951.

[29] M. Latorre-Sánchez, A. Primo, H. Garcia, *Angew. Chem. Int. Ed.* **2013**, *52*, 11813 – 11816; *Angew. Chem.* **2013**, *125*, 11813 – 11816.

[30] L. E. Heim, D. Thiel, C. Gedig, J. Deska, M. H. G. Prechtl, *Angew. Chem. Int. Ed.* **2015**, *54*, 10308 – 10312; *Angew. Chem.* **2015**, *127*, 10447 – 10451.

[31] Z. Liu, Z. Yin, C. Cox, M. Bosman, X. Qian, N. Li, H. Zhao, Y. Du, J. Li, D. G. Nocera, *Sci. Adv.* **2016**, *2*, e1501425.

[32] Y. Huang, X. Zhou, M. Yin, C. Liu, W. Xing, *Chem. Mater.* **2010**, *22*, 5122 – 5128.

[33] W. Wang, T. He, X. Liu, W. He, H. Cong, Y. Shen, L. Yan, X. Zhang, J. Zhang, X. Zhou, *ACS Appl. Mater. Interfaces* **2016**, *8*, 20839 – 20848.

[34] Y. Shen, Y. Zhan, S. Li, F. Ning, Y. Du, Y. Huang, T. He, X. Zhou, *Chem. Sci.* **2017**, *8*, 7498 – 7504.

[35] Y. — z. Wang, Z.-p. Zhao, M.-f. Li, Y.-z. Chen, W.-f. Liu, *J. Membr. Sci.* **2016**, *514*, 44 – 52.

[36] R. Obert, B. C. Dave, *J. Am. Chem. Soc.* **1999**, *121*, 12192 – 12193.

[37] Q. Sun, Y. Jiang, Z. Jiang, L. Zhang, X. Sun, J. Li, *Ind. Eng. Chem. Res.* **2009**, *48*, 4210 – 4215.

[38] A. Dibenedetto, P. Stufano, W. Macyk, T. Baran, C. Fragale, M. Costa, M. Aresta, *ChemSusChem* **2012**, *5*, 373 – 378.

[39] J. Shi, Y. Jiang, Z. Jiang, X. Wang, X. Wang, S. Zhang, P. Han, C. Yang, *Chem. Soc. Rev.* **2015**, *44*, 5981 – 6000.

[40] X. Zhou, Y. Huang, C. Liu, J. Liao, T. Lu, W. Xing, *ChemSusChem* **2010**, *3*, 1379 – 1382.

[41] J. Vorholt, *Arch. Microbiol.* **2002**, *178*, 239 – 249.

[42] Z. Wang, S. M. Lu, J. Li, J. Wang, C. Li, *Chem. Eur. J.* **2015**, *21*, 12592 – 12595.

[43] Y. Mao, Q. Kong, B. Guo, X. Fang, X. Guo, L. Shen, M. Armand, Z. Wang, L. Chen, *Energy Environ. Sci.* **2011**, *4*, 3442 – 3447.

[44] M. Sevilla, P. Valle-Vigon, A. B. Fuertes, *Adv. Funct. Mater.* **2011**, *21*, 2781 – 2787.

[45] Z. W. Seh, H. Wang, P.-C. Hsu, Q. Zhang, W. Li, G. Zheng, H. Yao, Y. Cui, *Energy Environ. Sci.* **2014**, *7*, 672 – 676.

[46] R. Aydın, H. Ö. Doğan, F. Köleli, *Appl. Catal. B* **2013**, *140*, 478 – 482.

[47] A. Mohammadi, I. Lundström, O. Inganäs, *Synth. Met.* **1991**, *41*, 381 – 384.

[48] L. Xia, G. Liu, J. Liu, M. Sun, *Kinet. Catal.* **2011**, *52*, 716 – 722.

[49] K. Jiang, K. Xu, S. Zou, W.-B. Cai, *J. Am. Chem. Soc.* **2014**, *136*, 4861 – 4864.

[50] E. A. Bielinski, P. O. Lagaditis, Y. Zhang, B. Q. Mercado, C. Würtele, W. H. Bernskoetter, N. Hazari, S. Schneider, *J. Am. Chem. Soc.* **2014**, *136*, 10234 – 10237.

↖↖ **These are not the final page numbers!**

FULL PAPERS

Y. Shen, Y. Zhan, S. Li, F. Ning, Y. Du,
Y. Huang, T. He, X. Zhou*

■■ – ■■

Methanol–Water Aqueous-Phase Reforming with the Assistance of Dehydrogenases at Near-Room Temperature

Enzyme time: A new strategy is designed to convert methanol into hydrogen at near-room temperature. This strategy involves two processes: $CH_3OH \rightarrow HCOOH \rightarrow H_2$ and $NADH \rightarrow HCOOH \rightarrow H_2$. This method is synergistically realized by enzymes and a chemical catalyst and provides inspiration for hydrogen production from other small organic molecules or biomass. FDH = formate dehydrogenase, Cp* = pentamethylcyclopentadienyl, ppy = polypyrrole.